2.04 µm Light Generation from a Ti:Sapphire Laser Using a Photonic Crystal Fiber with Low OH loss

Stephen A. Dekker[(1)], Alexander C. Judge[(1)], Ravi Pant[(1)], Itandehui Gris-Sánchez[(2)], Jonathan C. Knight[(2)], C. Martijn de Sterke[(1)], Benjamin J. Eggleton[(1)]

[(1)] *Centre for Ultrahigh-Bandwidth Devices for Optical Systems, Institute for Photonics and Optical Science, School of Physics, The University of Sydney, NSW 2006, Australia.*

[(2)] *Centre for Photonics and Photonic Materials, Dept. of Physics, University of Bath, Bath BA2 7AY, UK.*

Author email address: sdekker@physics.usyd.edu.au

Abstract: We report on the generation of 2.04 µm light from an 801 nm Ti:Sapphire source via soliton self-frequency shift and resonant dispersive wave emission in a PCF with low OH loss and broad anomalous dispersion region.

1. Introduction and Background

Applications for fiber optics in the mid-infrared (mid-IR) require sources in the wavelength range above 2 µm. This may be achieved by exploiting nonlinear processes to down-convert light from conventional sources at shorter wavelengths [1]. The soliton self-frequency shift (SSFS) [2] has been exploited in the realization of pulsed, wavelength tunable sources and, more generally, is a method for transferring light towards longer wavelengths. It occurs as a result of the red-shift induced by intra-pulse Raman scattering. There have been several demonstrations of the SSFS in different types of silica fiber [3-9]. The maximum shift achievable in these experiments is limited on the long wavelength side by the intrinsic absorption of silica at wavelengths above $\lambda \approx 2$ µm [4, 9]. Since the SSFS requires anomalous dispersion, the separation of the first and second zero-dispersion wavelengths (ZDWs), λ_{ZD1} and λ_{ZD2}, also limits the achievable red-shift. The λ_{ZD1} can be lowered by using Photonic Crystal Fibers (PCFs) with small cores, but this dramatically increases the OH loss peak around a wavelength $\lambda \approx 1400$ nm [10], thus creating an upper limit on the SSFS when pumping at shorter wavelengths.

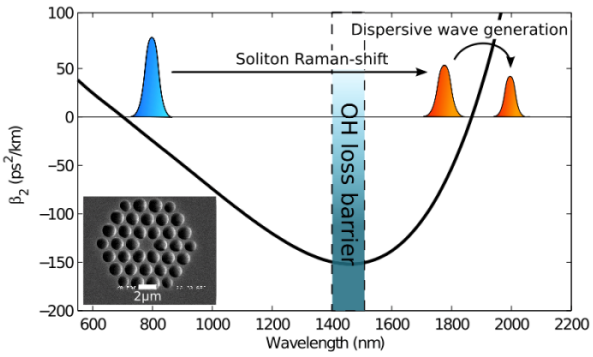

Fig. 1. Schematic of the soliton self-frequency shift showing an input soliton shifting from near the first zero-dispersion wavelength to the second zero-dispersion wavelength while crossing the traditional region of OH absorption. Dispersive waves are formed when the soliton approaches the second ZDW. Inset shows an SEM of the fiber core region.

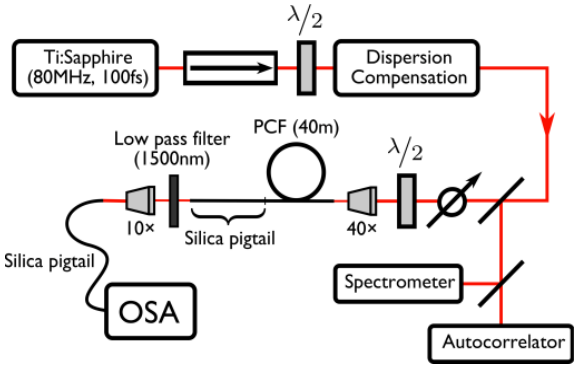

Fig. 2. Schematic of the experimental set-up: pulses from a mode-locked Ti:Sappire laser are coupled into 22 m of PCF, via an attenuator and a polarization controller. The output is analyzed on an OSA.

When a soliton approaches the second ZDW, the SSFS is halted, but leads to the generation of resonant dispersive waves (DWs) on the long wavelength side [11]. This process, along with the SSFS, enables an efficient redshift of energy from a short wavelength pump. For a given pump pulse, the extent of this red-shift depends largely upon the dispersion and losses of the fiber employed.

Here we present an experimental demonstration of light emission at 2040 nm through the efficient redshifting of light from a mode-locked Ti:Sapphire pump at 801 nm in a PCF. The measured photon conversion efficiency from the pump to the dispersive wave feature for this process is 3%, which corresponds to an average output power of 1.3 mW in the DW feature. This process is made possible by two key characteristics of our PCF, which was selected especially for the purpose of this experiment. First, it limits the OH loss to a maximum of 0.090 dB/m at 1380 nm.

Second, the zero-dispersion wavelengths λ_{ZD1} = 700 nm and λ_{ZD2} = 1870 nm are (i) widely spaced, while maintaining anomalous dispersion ($\beta_2 = -24$ ps^{2}km^{-1}) at the pump wavelength of 801 nm, and (ii) are at sufficiently short wavelengths so as not to be affected by infrared absorption.

The concept behind the redshifting process is shown schematically in Figure 1: the widely spaced ZDWs ensure a large wavelength range with anomalous dispersion, which, in principle, is available for the SSFS. In commercially available fibers with these parameters the high loss associated with the OH peak around a wavelength of 1400 nm prevents this full interval from being exploited. Additional red-shift of the soliton beyond the anomalous dispersion region is limited by the spectral recoil associated with the resonant emission by the soliton of "Cerenkov emission" [12], dispersive waves in the normal dispersion region when the soliton approaches λ_{ZD2}.

The fiber used in our experiments has a length of 40 m and a core diameter of 1.5 μm; an SEM of the cross section of the fiber core area is shown in the inset of Fig. 1. The peak OH-associated attenuation for this fiber is 0.09 dB/m. Using the SEM of the fiber cross-section and a commercially available finite-element software package, the anomalous dispersion region was calculated to range from λ_{ZD1} = 700 nm to λ_{ZD2} = 1870 nm, as shown in Fig. 1. This window, wherein the nonlinear coefficient is calculated to vary monotonically from $\gamma = 0.12$ (Wm)$^{-1}$ at λ_{ZD1} to $\gamma = 0.03$ (Wm)$^{-1}$ at λ_{ZD2}, permits an SSFS across almost the entire anomalous dispersion regime for an input wavelength of 801 nm.

2. Fiber fabrication

The fiber was fabricated using the stack-and-draw process but with additional steps to reduce spectral attenuation. Previously published data on attenuation in such small-core PCFs shows a strong increase in the spectral attenuation for core diameters below about 2 μm, due to extrinsic OH contamination during stacking, and structural damage to the silica matrix during the drawing. These together cause the increased attenuation both at the OH overtones and at other wavelengths within the transparency window of silica. Previous efforts to reduce these effects using halogen-based dehydration were only partially successful [13]. In our fibers we greatly reduced these effects by annealing the preform in a dry environment immediately prior to fiber drawing [14], which allowed us to fabricate low attenuation, small-core fibers with zero dispersion wavelengths suitable for a large SSFS in the near-IR.

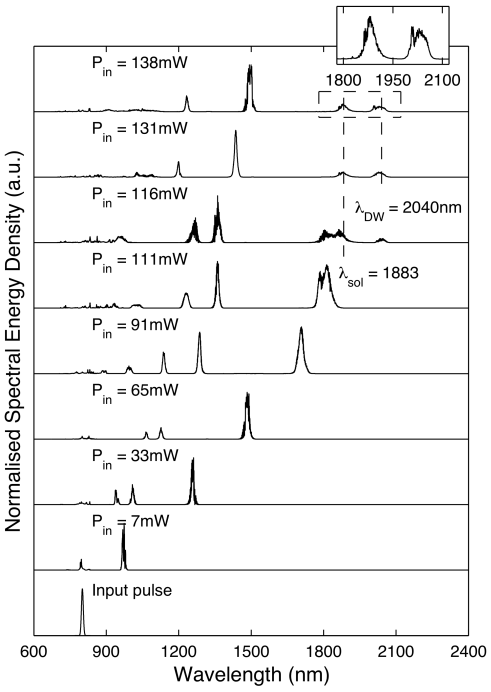

Fig. 3. PCF output spectra for a range of average input powers, with the input spectrum (bottom). Detail of the depleted soliton and DW enclosed in the dashed box is shown inset. λ_{sol} and λ_{DW} are indicated with vertical dashed lines.

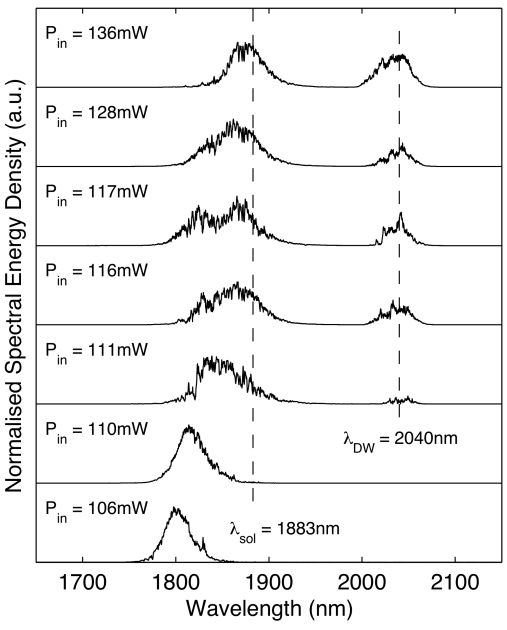

Fig. 4. Detail showing the spectrum of the depleted soliton and DW feature measured as a function of input average power. The vertical dashed lines indicate λ_{sol} and λ_{DW}.

3. Experiment and Results

The experimental setup is shown schematically in Figure 2. Pulses from a mode-locked Ti:Sapphire laser with a repetition rate of 83 MHz and centre wavelength of 801 nm were launched into the PCF using a 40× microscope objective. An optical isolator was used at the output of the laser to avoid disruptive feedback. The pulse had a full-width at half-maximum of 105 fs, as measured using an autocorrelator, and assuming a Gaussian pulse shape. Simultaneous measurements of the pulse spectrum showed that the pulse was close to transform limited.

Due to the birefringence of our PCF, a half-wave plate was used to choose the input polarization such that the red-shift was maximized at the highest input power. Subsequently, the input power was tuned using a variable attenuator and the output spectrum recorded using two optical spectrum analyzers (OSAs), an Ando AQ6317B covering the range from 600 nm to 1750 nm and a Yokogawa AQ6375 from 1400 nm to 2200 nm. A removable free-space, low-pass filter was placed between the output of the sample and the OSA when measuring wavelengths longer than 1500 nm to avoid spurious spectral features due to higher order diffraction effects. In the spectral region of overlap, the measurements of the two OSAs were largely consistent.

Figure 3 shows the output spectra for different input powers. The wavelength of the strongest soliton increases continuously as the input power varies from 7 mW to 116 mW. At a power of 91 mW, the dominant soliton in the output spectrum has a wavelength of λ = 1708 nm. For input powers exceeding 111 mW, the dominant soliton is disrupted by the proximity of λ_{ZD2}, while at 116 mW and above the red-shift starts to saturate at λ_{sol} = 1883 nm. A spectral feature then arises in the normal dispersion region at λ_{DW} = 2040 nm, corresponding to DWs shed by the soliton, as shown in detail in Figure 4.

We have ascertained that the energy at wavelengths shorter than the pump wavelength is negligible, so the spectra included here show essentially all of the output power. Thus, our experiments combine a very large SSFS with a high efficiency. The dispersive wave feature contains 8% of the photons incident on the fiber, representing around 3% and 13% of the incident and output powers, respectively.

4. Conclusions

In conclusion, we have demonstrated the generation of light at 2040 nm from an 801 nm pump, a ratio of well over 2.5, using a specially selected PCF with reduced OH loss. Using input powers above the threshold of 111 mW, we were able to induce emission of dispersive waves at λ_{DW} = 2040 nm, containing 3% of the total incident photons. Below this power level we generate solitons at a wavelength of up to approximately 1800 nm. This demonstration of the generation of radiation with a wavelength λ > 2 μm directly from a Ti:Sapphire laser, raises the possibility for the realization of novel mid-infrared sources.

References

[1] S. Zlatanovic, J. Park, S. Moro, J. Chavez Boggio, I. Divliansky, N. Alic, S. Mookherjea and S. Radic, "Mid-infrared wavelength conversion in silicon waveguides using ultracompact telecom-band-derived pump source," Nature Photon. **4**, 561 - 564 (2010).

[2] F. Mitschke and L. Mollenauer, "Discovery of the soliton self-frequency shift," Opt. Lett. **11**, 659–661 (1986).

[3] X. Liu, C. Xu, W. Knox, J. Chandalia, B. J. Eggleton, S. Kosinski, and R. Windeler, "Soliton self-frequency shift in a short tapered air–silica microstructure fiber," Opt. Lett. **26**, 358–360 (2001).

[4] N. Nishizawa and T. Goto, "Widely wavelength-tunable ultrashort pulse generation using polarization maintaining optical fibers," IEEE J. Sel. Top. Quantum Electron. **7**, 518–524 (2001).

[5] S. Kobtsev, S. Kukarin, N. Fateev, and S. Smirnov, "Generation of self-frequency-shifted solitons in tapered fibers in the presence of femtosecond pumping," Laser Phys. **14**, 748–751 (2004).

[6] N. Ishii, C. Teisset, S. Köhler, E. Serebryannikov, T. Fuji, T. Metzger, F. Krausz, A. Baltuška, and A. Zheltikov, "Widely tunable soliton frequency shifting of few-cycle laser pulses," Phys. Rev. E **74**, 36617 (2006).

[7] J. Takayanagi, T. Sugiura, M. Yoshida, and N. Nishizawa, "1.0–1.7-μm wavelength-tunable ultrashort-pulse generation using femtosecond Yb-doped fiber laser and photonic crystal fiber," IEEE Photon. Technol. Lett. **18**, 21 (2006).

[8] J. van Howe, J. Lee, S. Zhou, F. Wise, C. Xu, S. Ramachandran, S. Ghalmi, and M. Yan, "Demonstration of soliton self-frequency shift below 1300 nm in higher-order mode, solid silica-based fiber," Opt. Lett. **32**, 340–342 (2007).

[9] M. Chan, S. Chia, T. Liu, T. Tsai, M. Ho, A. Ivanov, A. Zheltikov, J. Liu, H. Liu, and C. Sun, "1.2-2.2-μm tunable Raman soliton source based on a Cr: Forsterite-laser and a photonic-crystal fiber," IEEE Photon. Technol. Lett. **20**, 900–902 (2008).

[10] L. Fu, B. Thomas, and L. Dong, "Small core ultra high numerical aperture fibers with very high nonlinearity," in "Conference on Lasers and Electro-Optics/Quantum Electronics and Laser Science Conference and Photonic Applications Systems Technologies," (Optical Society of America, 2008), p. CThV4.

[11] D. Skryabin, F. Luan, J. Knight, and P. Russell, "Soliton self-frequency shift cancellation in photonic crystal fibers," Science **301**, 1705 (2003).

[12] N. Akhmediev and M. Karlsson, "Cherenkov radiation emitted by solitons in optical fibers," Phys. Rev. A **51**, 2602–2607 (1995).

[13] A. Monteville. D. Landais, O. Goffic, D. Tregoat, N. Traynor, T. Nguyen, S. Lobo, T. Chartier, and J. Simon, "Low loss, low OH, highly non-linear holey fiber for Raman amplification," in "Conference on Lasers and Electro-Optics/Quantum Electronics and Laser Science Conference and Photonic Applications Systems Technologies," (Optical Society of America, 2006), p. CMC1.

[14] I. Gris-Sánchez, B.J. Mangan and J.C. Knight, "Reducing spectral attenuation in small-core photonic crystal fibers," Optical Materials Express, in press.